Published in final edited form as:
FEBS J. 2011 April ; 278(7): 1112–1125. doi:10.1111/j.1742-4658.2011.08026.x.

Modulation of F_0F_1-ATP synthase activity by cyclophilin D regulates matrix adenine nucleotide levels

Christos Chinopoulos[1,2], **Csaba Konràd**[2], **Gergely Kiss**[2], **Eugeniy Metelkin**[3], **Beata Töröcsik**[2], **Steven F. Zhang**[1], and **Anatoly A. Starkov**[1]

[1]Weill Medical College Cornell University, New York, NY, 10021, USA

[2]Department of Medical Biochemistry, Semmelweis University, Budapest, 1094, Hungary

[3]Institute for Systems Biology SPb, Moscow, Russia

Abstract

Cyclophilin D was recently shown to bind to and decrease the activity of F_0F_1-ATP synthase in submitochondrial particles and permeabilized mitochondria (Giorgio et al. 2009, J Biol Chem, 284:33982). Cyclophilin D binding decreased both the ATP synthesis and hydrolysis rates. Here, we reaffirm these findings by demonstrating that in intact mouse liver mitochondria energized by ATP, absence of cyclophilin D or presence of cyclosporin A led to a decrease in the extent of uncoupler-induced depolarization. Accordingly, in substrate-energized mitochondria an increase in F_0F_1-ATP synthase activity mediated by a relief of inhibition by cyclophilin D was evident as slightly increased respiration rates during arsenolysis. However, the modulation of F_0F_1-ATP synthase by cyclophilin D did not increase the ANT-mediated ATP efflux rate in energized mitochondria or the ATP influx rate in de-energized mitochondria. The lack of effect of cyclophilin D on the ANT-mediated adenine nucleotide exchange rate was attributed to the ~2.2 times lower flux control coefficient of the F_0F_1-ATP synthase than that of ANT, deduced from measurements of adenine nucleotide flux rates in intact mitochondria. These findings were further supported by a recent kinetic model of the mitochondrial phosphorylation system, suggesting that a ~30% change in F_0F_1-ATP synthase activity in fully energized or fully deenergized mitochondria affects ADP-ATP exchange rate mediated by the ANT in the range of 1.38-1.7%. We conclude that in mitochondria exhibiting intact inner membranes, the absence of cyclophilin D or inhibition of its binding to F_0F_1-ATP synthase by cyclosporin A will affect only matrix adenine nucleotides levels.

Keywords

arsenate; adenine nucleotide translocase; adenine nucleotide translocator; adenine nucleotide carrier; permeability transition pore; control strength; metabolic control analysis; kinetic model; systems biology; phosphate carrier; co-precipitation

INTRODUCTION

Mitochondrial bioenergetic functions rely exclusively on compartmentalization, demanding an intact inner mitochondrial membrane for the development of protonmotive force. It is therefore, not surprising that loss of mitochondrial membrane integrity is energetically

Address for correspondence: Dr. Anatoly A. Starkov, PhD, Weill Medical College Cornell University, 585 68th Street, A501, New York, NY 10021. Tel: +212-746-4534. ans2024@med.cornell.edu.

deleterious for cells. For reasons that are incompletely understood, mitochondria possess intrinsic mechanisms for doing exactly that, recruiting specific proteins to form a pore and disrupt inner mitochondrial membrane integrity. This pore, termed “permeability transition pore” (PTP) [1;2], is of a sufficient size (cut-off ~1,5 kDa) to allow the passage of solutes and water, that may also result in rupture of the outer membrane. The identity of the proteins comprising the PTP is debated; the ubiquitous matrix-located protein cyclophilin D (CYPD) is involved in the modulation of PTP open/closed probability. CYPD is a member of the cyclophilins family encoded by the *ppif* gene [3], that exhibit peptidyl-prolyl *cis/trans* isomerase activity. Inhibition of CYPD by cyclosporin A, or genetic ablation of the *ppif* gene [4-7], negatively affect the PTP opening probability. CYPD inhibition or its genetic ablation exhibit an unquestionable inhibitory effect on PTP in mitochondria isolated from responsive tissues. However, apart from the recent finding by Basso and colleagues showing that ablation of CYPD or treatment with cyclosporin A does not directly cause PTP inhibition, but rather unmasks an inhibitory side for P_i [8], the *modus operandi* of CYPD in promoting pore opening is incompletely understood. It is not clear if the *cis-trans* peptidyl prolyl isomerase activity is required for promoting PTP [9;10]. Furthermore, transgenic mice that constitutively lack CYPD do not exhibit a severe phenotype that could manifest in view of a major bioenergetic insufficiency. Instead, these mice exhibit an enhancement of anxiety, facilitation of avoidance behavior, occurrence of adult-onset obesity [11] and a defect in platelet activation and thrombosis [12]. However, CYPD-knock-out mice score better compared to WT littermates in mouse models of Alzheimer’s disease [13] muscular dystrophy [14], and acute tissue damage induced by a stroke or toxins [4-7]. Furthermore, genetic ablation of CYPD or its inhibition by cyclosporin A or Debio 025 rescues mitochondrial defects and prevents muscle apoptosis in mice suffering from collagen VI myopathy [15-17]. The beneficial effects of cyclosporin A has also been demonstrated in patients suffering from this type of myopathy [18]. Unlike the clear implication of CYPD in diverse pathologies, it is not yet known what the physiological action of this protein in mitochondria is.

Recently, Giorgio et al reported [19] that CYPD binds to the lateral stalk of the F_0F_1-ATP synthase in a phosphate-dependent manner, resulting in a decrease in both ATP synthesis and hydrolysis mode of this complex. Genetic ablation of the *ppif* gene or inhibition of CYPD binding on F_0F_1-ATP synthase by cyclosporin A, led to a disinhibition of the ATPase, resulting in accelerated ATP synthesis and hydrolysis rates.

However, these effects were demonstrated in either submitochondrial particles, or mitochondria permeabilized by alamethicin, conditions in which there is a direct access to the F_0F_1-ATP synthase. In intact mitochondria, changes in ATP synthesis or hydrolysis rates by the F_0F_1-ATP synthase do not necessarily translate to changes in ATP efflux or influx rates, due to the presence of the adenine nucleotide translocase (ANT). The molecular turnover numbers and the number of active ANT molecules may vary from those of F_0F_1-ATP synthase molecules per mitochondrion [20;21]. Furthermore, the steady-state ADP-ATP exchange rates (for ANT) or ADP-ATP conversion rates (for F_0F_1-ATP synthase) do not change in parallel as a function of the mitochondrial transmembrane potential ($\Delta\Psi m$) [22;23]. It is therefore reasonable to assume, that a change in matrix ADP-ATP conversion rate caused by a change in F_0F_1-ATP synthase activity may not result in an altered rate of ADP influx (or ATP influx, in case of sufficiently deenergized mitochondria) from the extramitochondrial compartment, due to the imposing action of the ANT. The purpose of the present work was to address the extent of contribution of CYPD on rates of ADP and ATP fluxes towards the extramitochondrial compartment. We report that for as long as the inner mitochondrial membrane integrity remained intact, the absence of CYPD or its inhibition by cyclosporin A did not affect the ATP efflux rate in energized mitochondria or the rate of ATP consumption in deenergized mitochondria. However, the absence of CYPD or its

inhibition by cyclosporin A significantly enhanced the rate of F_0F_1-ATP synthase-mediated regeneration of ATP consumed by arsenolysis in the matrix and decreased the extent of uncoupler-induced depolarization in ATP-energized intact mitochondria. Functional results obtained here are supported by the finding that the CYPD-F_0F_1-ATP synthase interaction was demonstrated in intact mitochondria using the membrane-permeable cross-linker, 3-3'-dithiobis[sulfosuccinimidylpropionate], (DSP) followed by co-precipitation using an antibody for F_0F_1-ATP synthase as bait; cyclosporin A was found to diminish the binding of CYPD on the ATP synthase. Our results indicate that modulation of F_0F_1-ATP synthase activity by CYPD comprises an "in-house" mechanism of regulating matrix adenine nucleotide levels that does not transduce to the extramitochondrial compartment for as long as the inner mitochondrial membrane remains intact.

RESULTS

ADP-ATP exchange rates in intact mitochondria and ATP hydrolysis rates in permeabilized mitochondria

ADP-ATP exchange rate mediated by the ANT in mitochondria is influenced by ΔΨm [20;22;24-27], among many other parameters, as elaborated below and in reference [22]. We investigated the ADP-ATP exchange rate mediated by the ANT in intact isolated WT and CYPD KO mouse liver mitochondria, both in the presence and absence of cyclosporin A, in the -130 -160 mV ΔΨm range, titrated by the uncoupler SF 6847 using different concentrations, and at 0 mV produced by a maximal dose of the uncoupler. We compared these ADP-ATP exchange rates mediated by the ANT to those obtained by direct ATP hydrolysis rates by the F_0F_1-ATP synthase in mitochondria that have been permeabilized by alamethicin.

Mitochondria were energized by succinate (5 mM) and glutamate (1 mM) in order to disfavor matrix substrate-level phosphorylation; glutamate could enter the citric acid cycle through conversion to α-ketoglutarate, and get converted by the α-ketoglutarate dehydrogenase complex to succinyl-CoA, that would in turn be converted to succinate plus ATP by succinate thiokinase. This amount of ATP could contribute to ATP efflux from mitochondria [23]. The disfavoring of glutamate supporting substrate-level phosphorylation was secured by the high concentration of succinate that keeps the reversible succinate thiokinase reaction towards succinyl-CoA plus ADP plus P_i formation. This is reflected by the fact that in the presence of glutamate and succinate, α-ketoglutarate is primarily exported out of mitochondria [28] while succinate almost completely suppresses the oxidation of NAD^+-linked substrates, at least in partially inhibited State 3 and in State 4 [29]. Furthermore, succinate suppresses glutamate deamination [30]. The lack of oxidation of 1 mM glutamate in the presence of 5 mM succinate can be demonstrated by the complete lack of effect of rotenone on recordings of membrane potential from mitochondria energized by this substrate combination during state 3 respiration (not shown).

ADP was added (2 mM), and small amounts of the uncoupler SF 6847 was subsequently added (10-30 nM) in order to reduce ΔΨm to not more than -130 mV, while ΔΨm was recorded as time courses from fluorescence changes due to redistribution of safranine O across the inner mitochondrial membrane. In parallel experiments, ATP efflux rates were calculated from measuring extramitochondrial changes in free [Mg^{2+}], by the recently described method by Chinopoulos et al [20], exploiting the differential affinity of ADP and ATP to Mg^{2+} (see under Materials and Methods). ADP-ATP exchange rates as a function of ΔΨm in the -130 -160 mV range, comparing mitochondria isolated from the livers of WT versus CYPD KO mice is shown in figure 1, panel A. As shown, there was no difference in ATP efflux-ΔΨm profile of the WT compared to CYPD KO mice, while ANT was operating in the forward mode. Likewise, when mitochondria were completely depolarized by 1 μM

SF 6847 (figure 1, panel B), no statistical significant difference was observed between mitochondria isolated from WT and CYPD KO mice during ATP influx, irrespective of the presence of cyclosporin A (1 μM) in the medium. However, if mitochondria were subsequently permeabilized by alamethicin (20 μg), mitochondria isolated from CYPD KO mice exhibited a 30.9 ± 1.3% faster ATP hydrolysis rate than WT littermates. The effect of cyclosporin A (1 μM) was only 14.3 %, but nonetheless, statistically significant (p=0.027). This ATP hydrolysis rate was 96.7% sensitive to oligomycin, thus affording the assumption that it was almost entirely due to the F_0F_1-ATP synthase.

In order to provide further assurance that in intact mitochondria the binding of CYPD to F_0F_1-ATP synthase occurs and is inhibitable by cyclosporin A we incubated mitochondria with the membrane-permeable cross-linker DSP in the absence or presence of cys A, extracted proteins with 1% digitonin [19], immunoprecipitated with anti Complex V antibodies, and finally tested immunocaptured proteins for the presence of CYPD using the β subunit of the F_0F_1-ATP synthase as loading control. As shown in figure 1, panel D, digitonin-treated, cross-linked samples pulled down CYPD (lane 3), and cys A reduced the amount of CYPD bound to F_0F_1-ATP synthase (lane 4). In lane 1, mitochondria from the liver of a CYPD-WT mouse and in lane 2 mitochondria from the liver of a CYPD-KO mouse were loaded (0.85 μgr each), serving as a positive and negative control for the CYPD blot, respectively. It is to be noted that only in the immunoprecipitates a band of higher molecular weight than CYPD was present, most likely due to reaction of the secondary antibody with the light chains of the immunoglobulins used for immunoprecipitation. From the results shown in panel D of figure 1, we deduce that the CYPD- F_0F_1-ATP synthase interactions can be observed in intact mitochondria, and that cys A disrupts these interactions.

Prediction of alterations in ADP-ATP exchange rate mediated by the ANT caused by alterations in matrix ATP and ADP levels, due to changes in F_0F_1-ATP synthase activity by kinetic modeling

The rate equation of electrogenic translocation of adenine nucleotides catalyzed by the ANT (V_{ANT}) has been derived in [27] and implemented in a complete mitochondrial phosphorylation system in [22]:

$$\nu_{ANT}=c_{ANT}\cdot\frac{1}{\Delta^{ANT}}\left(k_2^{ANT}q^{ANT}\frac{T_i\cdot D_o}{K_{Do}^{ANT}}-k_3^{ANT}\frac{D_i\cdot T_i}{K_{To}^{ANT}}\right),$$
$$\Delta^{ANT}=\left(1+\frac{T_o}{K_{To}^{ANT}}+\frac{D_o}{K_{Do}^{ANT}}\right)\left(D_i+q^{ANT}\cdot T_i\right), \quad \text{Eq. 1}$$

here,

$$q^{ANT}=\frac{k_3^{ANT}K_{Do}^{ANT}}{k_2^{ANT}K_{To}^{ANT}}\exp(\phi),$$
$$K_{Do}^{ANT}=K_{Do}^{ANT,0}\exp(3\delta_D\phi),$$
$$K_{To}^{ANT}=K_{To}^{ANT,0}\exp(4\delta_T\phi),$$
$$k_2^{ANT}=k_2^{ANT,0}\exp\{(-3a_1-4a_2+a_3)\phi\},$$
$$k_3^{ANT}=k_3^{ANT,0}\exp\{(-4a_1-3a_2+a_3)\phi\}$$

Likewise, the rate equation of the F_0F_1-ATP synthase reaction (V_{SYN}) has been derived in [31;32] and implemented in a complete mitochondrial phosphorylation system in [22]:

$$V_{SYN} = c_{SYN} \cdot V_{\max}^{SYN} \exp(n_{SYN}\chi\phi)\left(\frac{H_o}{K_{Ho}^{SYN}}\right)^{n_{SYN}} \times \times \frac{1}{K_{MgD}^{SYN} \cdot K_{P1}^{SYN}} \frac{MgD_i \cdot P1_i - MgT_i \cdot K_{eq}^{SYN} \cdot \exp(-n\phi)\cdot\left(\frac{H_o}{H_i}\right)^{-n}}{1+\frac{MgD_i \cdot P1_i}{K_{MgD}^{SYN} \cdot K_{P1_i}^{SYN}}\left(\frac{H_o}{K_{Ho}^{SYN}}\right)^{n_{SYN}} + \frac{MgT_i}{K_{MgT}^{SYN}}\left(\frac{H_i}{K_{Hi}^{SYN}\exp(\chi n\phi)}\right)^{n_{SYN}}} \quad \text{Eq.2}$$

Here, $\phi = -\frac{F\Delta\psi}{RT}$ and $K_{eq}^{SYN} = K_{hyd}^{SYN}\frac{K_{T,Mg}}{K_{D,Mg}} \cdot \frac{10^{-7+3}}{10^{-7+3}+K_{P,H}}$

Values and explanations of all parameters of equations 1 and 2 are taken from [22] and [27] and references therein. T_i and D_i indicate free matrix ATP and ADP concentrations, respectively, while T_o and D_o indicate free extramitochondrial ATP and ADP concentrations, respectively. These equations form two out of the three ordinary differential equations that model ATP-ADP steady-state exchange rate in intact isolated mitochondria; the third component being the phosphate carrier. The model reproduces experimental results with the assumption that the phosphate carrier functions under “rapid equilibrium” [22]. As seen in equations 1 and 2 and reference [22], the ADP-ATP exchange rate mediated by the ANT and the F_0F_1-ATP synthase activity depend on the common terms T_i and D_i. We were therefore able to calculate the changes in T_i and D_i, assuming an increase in F_0F_1-ATP synthase activity by 30%, (due to CYPD ablation), and estimate the impact on ADP-ATP exchange rate mediated by the ANT for predefined values of ΔΨm. Such values of ΔΨm were chosen, as depicted in figure 1A, that were obtained by addition of the uncoupler SF 6847 in different concentrations. The results of the calculations are shown in table 1. As seen in table 1, the increase in ADP-ATP exchange rate mediated by the ANT due to a 30% increase in F_0F_1-ATP synthase activity is in the range of 1.38-7.7%. Percentage change increased for more depolarized ΔΨm values, approaching the reversal potential of the ANT [23]. At 0 mV, during which both the ANT and the F_0F_1-ATP synthase operate in reverse mode, the increase in ADP-ATP exchange rate mediated by the ANT drops to 1.7%. It is to be noted, that the greatest increase in ADP-ATP exchange rate mediated by the ANT calculated at -134 mV (7.7%) occurs during the lowest ADP-ATP exchange rate (figure 1A). It is therefore, least likely to observe a statistical significance in adenine nucleotide flux rates from mitochondria obtained from WT versus CYPD KO littermates. The above calculations afford the assumption that a 30% increase in F_0F_1-ATP synthase activity will lead to an insignificant increase (1.38-1.7%) in ADP-ATP exchange rate mediated by the ANT, in maximally polarized (forward mode of both ANT and ATPase) and maximally depolarized (reverse mode of both ANT and ATPase) mitochondria.

Flux control coefficients of ANT and F_0F_1-ATP synthase for adenine nucleotide flux rates

The above calculations are a product of a validated model. In order to strengthen the predictions of the model with experimental evidence on the pertaining conditions, we measured the flux control coefficients of the reactions catalyzed by the ANT and the F_0F_1-ATP synthase separately, on ADP-ATP flux rates from energized intact mitochondria. This coefficient is defined, for infinitesimally small changes, as the percent change in the steady state rate of the pathway divided by the percent change in the enzyme activity causing the flux change. The flux control coefficient for ANT and most other mitochondrial bioenergetic entities have been measured in a variety of conditions, but on respiration rates, not adenine nucleotide flux rates [33-48]. Although no individual step was found to be ‘rate-limiting’ (i.e. having a flux control coefficient equal to 1) [33;39;45;49], the regulatory potential of any particular step is quantitated by its control coefficient. During State 3, ANT exhibits a control coefficient of ~0.4 [38;40;46], for respiration rates. At 10 mM extramitochondrial P_i,

the phosphate carrier exhibits a flux control coefficient of <0.1, and this is also reflected by the predictions of the model assuming that the carrier operates in rapid equilibrium.

The model predictions shown above would be strengthened if the flux control coefficient of the ANT is sufficiently higher than that of the F_0F_1-ATP synthase, for adenine nucleotide flux rates. The determination of the flux control coefficients (FCCs) was performed by measuring ATP efflux rates, correlating it to the difference of ΔΨm (termed Delta phi) before and after addition of ADP (2 mM) to WT and CYPD KO mitochondria, and calculated on the basis of steady-state titration data by catr and olgm. The activities of ANT and F_0F_1-ATP synthase were calculated taking into account the strong irreversible inhibition of ANT and F_0F_1-ATP synthase by their respective inhibitors [50-53]:

$$a_{ANT} = \frac{CATRm - CATR}{CATRm},$$

where *CATR* is the concentration of CATR added, *CATRm* is the minimal concentration of CATR that corresponds to maximum ANT inhibition (205 nM of CATR). a_{ANT} is the activity of ANT normalized to initial activity (from 0 to 1). A similar equation was used for F_0F_1-ATP synthase activity performing calculations with 35 nM of olgm for OLGMm.

$$a_{ATPsyn} = \frac{OLGMm - OLGM}{OLGMm}$$

The logarithmic values of ATP flux vs. activities were plotted as shown in panel C of figure 2 and analyzed by linear regression. The FCC values were estimated as the coefficients of the linear regression according to the definition: $FCC_{ANT} = \frac{\partial \ln (V_{ANT})}{\partial \ln (a_{ANT})}$, and likewise for the F_0F_1-ATP synthase.

A similar ADP/ATP exchange rate versus ΔΨm profile had been observed in rat liver mitochondria, shown in [23]. The calculated FCC values are shown in panel D of figure 2. As shown, the FCC of both WT and CYPD KO ANT is ~2.2 times higher than that of the F_0F_1-ATP synthase.

Effect of altering matrix pH on adenine nucleotide exchange rates

It can be argued, that since the uncoupler acidified the matrix, this may have directly affected CYPD binding to the inner membrane by means of decreasing matrix P*i* concentration –which could in turn affect CYPD binding to F_0F_1-ATP synthase- and decreased binding of the inhibitory protein IF-1 to ATPase. IF1 is a naturally occurring protein that inhibits the consumption of ATP by a reverse-operating F_0F_1-ATP synthase [54;55], especially during acidic conditions [56;57]. IF1 would inhibit ATP hydrolysis independent of the CYPD- F_0F_1-ATP synthase interaction, and as such mask activation of ATP hydrolysis due to CYPD ablation or displacement by cyclosporin A. ΔpH across the inner mitochondrial membrane is inversely related to the amount of Pi in the medium [20;58-60], and in the presence of abundant P_i, ΔpH is in the 0.11-0.15 range [61;62]. Accordingly, at pH_o=7.25, pH_{in} in our hands was 7.39 +/- 0.01, far from the 6.8 pH optimum of IF1. However, IF-1 also binds to the F_0F_1-ATP synthase at pH higher than 6.8, promoting the dimerization of two synthase units [55;63], thus modulating ATP synthesis [64]. Therefore, we manipulated matrix pH during the application of the uncoupler, and recorded ATP influx and efflux rates. The acidification produced by the uncoupler was either minimized by methylamine (60 μM), or exacerbated by nigericin (1 μM), as also

described in [61]. Matrix pH is shown in the white boxes within the grey bars, for the conditions indicated in the x-axis of the figure 3. As seen in figure 3B, ATP consumption rates were not statistically significantly different between WT and CYPD KO mitochondria, in which the uncoupler-induced acidification has been altered by either methylamine or nigericin (n=8, for all data bars). No differences were also observed for ATP efflux rates, in fully polarized mitochondria (figure 3A). The effect of nigericin decreasing ATP efflux rate in mitochondria even though it yielded a higher membrane potential (at the expense of ΔpH) has been explained in [22]. Methylamine did not affect ΔΨm (not shown), though in the concomitant presence of SF 6847, it decreased ATP consumption rates as compared to the effect of SF 6847 alone (figure 3B). Nigericin also decreased ATP consumption rates (figure 3B). The latter two effects were not further investigated.

CYPD decreases reverse H^+ pumping rate through the F_0F_1-ATPase in partially energized intact mitochondria

In order to demonstrate the ability of CYPD to modulate F_0F_1-ATP synthase -mediated ATP hydrolysis rates, we de-energized intact mouse liver mitochondria by substrate deprivation in the presence of rotenone, followed by addition of 2 mM ATP, while recording ΔΨm and compared the WT ± cyclosporin A versus CYPD KO mice. Under these conditions, due to the sufficiently low ΔΨm values prior to ATP addition, ANT and F_0F_1-ATP synthase operate in the reverse mode. Provision of exogenous ATP leads to ATP influx to mitochondria, followed by its hydrolysis by the reversed F_0F_1-ATP synthase that in turn pumps protons to the extramitochondrial compartment, establishing ΔΨm to an appreciable extent. In this setting, the ability of the F_0F_1-ATP synthase to pump protons out of the matrix represents the only component opposing the action of an uncoupler. Due to the recent report by the groups of Lippe and Bernardi [19] showing that the binding of CYPD to F_0F_1-ATP synthase occurs only in the presence of phosphate, we performed the below experiments in the presence and absence of 10 mM P_i. As shown in figure 4 panel A, in the presence of 10 mM P_i, mitochondria isolated from the livers of CYPD KO mice resisted more the uncoupler-induced depolarization (open quadrangles), than those obtained from WT littermates (open circles). Cyclosporin A also exhibited a similar effect on WT mitochondria (open triangles) but not on KO mice (not shown). These results also attests to the fact that a possible acidification-mediated IF1 binding on F_0F_1-ATP synthase, in turn masking the relief of inhibition by CYPD, could not account for the lack of effect on adenine nucleotide flux rates in intact mitochondria, as shown above. In the absence of exogenously added P_i, this effect was much less pronounced, figure 4 panel B; however, during endogenous ATP hydrolysis in intact mitochondria, it is anticipated that there can be a significant production of P_i in the vicinity of the ATPase within the matrix.

CYPD ablation or its inhibition by Cyclosporin A increases the rate of respiration stimulated by arsenate in intact mitochondria

Regarding the CYPD–F_0F_1-ATP synthase interaction and how it affects the efficiency of oxidative phosphorylation, we measured mitochondria respiration. CYPD ablation or inhibiting the CYPD with cyclosporin A had no effect on State 4 and State 3 respiration rates and did not affect ADP:O and respiratory control ratios (data not shown). Therefore, CYPD interaction with F_0F_1-ATP synthase does not translate to changes in the efficiency of oxidative phosphorylation of exogenously added ADP. However, it still may affect the phosphorylation state of endogenous adenine nucleotides present in the matrix of mitochondria. To test this hypothesis, we investigated the effect of AsO_4 on the rate of respiration of CYPD KO and WT mitochondria. This approach is based on a well-studied "uncoupling" effect of AsO_4 explained by its ability to substitute for P*i* in the F_0F_1-ATP synthase catalyzed reaction of phosphorylation of ADP. However, the AsO_3-ADP bond is easily and non-enzymatically water-hydrolysable, which forces a futile cycle of

phosphorylation of matrix ADP by F_0F_1-ATP synthase and stimulates respiration, [65] [66;67]. In these experiments, mitochondria were resuspended in a buffer as described in "Materials and Methods" supplemented with substrates and 0.2 mM EGTA but without Pi and ADP. AsO_4 was titrated to produce the maximum stimulation of the State 4 respiration, which was observed at 4 mM AsO_4. The maximum rate of oxygen consumption was obtained by supplementing the respiration medium with 400 nmol ADP. We found that CYPD KO mitochondria exhibited ~10% higher rates of AsO_4 stimulated respiration than WT mitochondria, with no changes in the maximum rates of respiration. As anticipated, a similar effect was observed with WT mitochondria treated with cyclosporin A, which stimulated their AsO_4-stimulated respiration to the level of CYPD KO mitochondria. (Table 2).

DISCUSSION

The present work extends the results obtained by the groups of Lippe and Bernardi demonstrating that changes in ATP synthesis or hydrolysis rates of the F_0F_1-ATP synthase due to CYPD binding does not translate to changes in ADP-ATP flux rates, even though CYPD binding on the F_0F_1-ATP synthase and unbinding by cys A was hereby demonstrated in intact mitochondria. This is due to an imposing role of the ANT. Apparently, the ADP-ATP exchange rates by the ANT are slower than the ADP-ATP interconversions by the F_0F_1-ATP synthase, an assumption which is afforded by the more than twice larger flux control coefficient of ANT (0.63 for WT, 0.66 for CYPD KO) than that of the F_0F_1-ATP synthase (0.29 for WT, 0.3 for CYPD KO), for adenine nucleotide flux rates. This is also supported by early findings from pioneers in the field, showing that the ANT is the step with the highest flux control coefficient in the phosphorylation of externally added ADP to energized mitochondria [68], and references therein. However, one could argue that a 30% change in F_0F_1-ATP synthase activity which exhibits a ~0.3 flux control coefficient, would alter adenine nucleotide exchange rates in intact mitochondria by $0.3\times0.3=0.09$, i.e. 9%. To this we must stress that the flux control coefficient applies for infinitesimally small changes in the percent change in the steady state rate of the pathway; if changes are large (e.g. 30%), the flux control coefficient decreases by a factor of ~5, or more [49;69]. Thereby, a 30% change in F_0F_1-ATP synthase activity translates to a $0.3\times0.3\times0.2=0.018$ or less, i.e. 1.8% difference in adenine nucleotide exchange rates in intact mitochondria. This is in good agreement with the predictions of the kinetic modeling, suggesting that a 30% increase in F_0F_1-ATP synthase activity yields a 1.38-1.7% increase in ADP-ATP exchange rate mediated by the ANT in fully polarized or fully depolarized mitochondria. Yet, in substrate-energized mitochondria an increase in ATP synthesis rate by relieving the inhibition of the F_0F_1-ATP synthase by CYPD was reflected by an increase in respiration rates during arsenolysis; likewise, in ATP-energized mitochondria with a non-functional respiratory chain, abolition of CYPD or its inhibition by cyclosporin A resulted in an accelerated ATP hydrolysis rate, allowing intact mitochondria to maintain a higher membrane potential.

The present findings imply that the modulation of F_0F_1-ATP synthase activity by CYPD comprises an "in-house" mechanism of regulating matrix adenine nucleotide levels, that does not transduce outside mitochondria, without evoking a functional correlation between CYPD and ANT due to a possible direct link [70].

This is the first documented example of an intramitochondrial mechanism of adenine nucleotide level regulation, that is not reflected in the extramitochondrial compartment. Furthermore, we speculate that cyclosporin A or *ppif* genetic ablation delays pore opening by providing a more robust $\Delta\Psi m$. It is well established that the lower the $\Delta\Psi m$, the higher the probability for pore opening [60;71-73]. In energized mitochondria, abolition of CYPD or its inhibition by cyclosporin A would lead to an accelerated ATP synthesis, while in

sufficiently depolarized mitochondria would result in accelerated proton pumping by ATP hydrolysis. However, an alternative explanation relates to matrix P_i which is a product of ATP hydrolysis by a reversed F_0F_1-ATP synthase, and inhibits PTP [8].It is therefore also reasonable to speculate that in deenergized mitochondria an increase in matrix P_i concentration could mediate the effect of cyclosporin A or CYPD genetic ablation in delaying PTP opening [8].

MATERIALS AND METHODS

Isolation of mitochondria from mouse liver

CYPD knock-out mice and wild-type littermates were a kind gift from Dr. Anna Schinzel [6]. Mitochondria from the livers of wild-type and CYPD knock-out littermate mice were isolated as detailed previously [74], with minor modifications. All experiments were carried out in compliance with the National Institute of Health guide for the care and use of laboratory animals and were approved by the Institutional Animal Care and Use Committee of Cornell University. Mice were sacrificed by decapitation and livers were rapidly removed, minced, washed and homogenized using a Teflon–glass homogenizer in ice-cold isolation buffer containing 225 mM mannitol, 75 mM sucrose, 5 mM Hepes, 1 mM EGTA, and 1 mg/ml bovine serum albumin (BSA) essentially fatty acid-free, with the pH adjusted to 7.4 with KOH. The homogenate was centrifuged at 1,250 g for 10 min; the pellet was discarded, and the supernatant was centrifuged at 10,000 g for 10 min; this step was repeated once. At the end of the second centrifugation, the supernatant was discarded, and the pellet was suspended in 0.15 ml of the same buffer with 0.1 mM EGTA. The mitochondrial protein concentration was determined using the bicinchoninic acid assay [75].

$[Mg^{2+}]_f$ determination from Magnesium Green fluorescence in the extramitochondrial volume of isolated mitochondria and conversion to ADP-ATP exchange rate

Mitochondria (1 mg, wet weight, in this and all subsequent experiments wet weight of mitochondrial amount is implied) were added to 2 ml of an incubation medium containing (in mM): KCl 8, K-gluconate 110, NaCl 10, Hepes 10, KH_2PO_4 10 (where indicated), EGTA 0.005, mannitol 10, $MgCl_2$ 0.5 (or 1, where indicated), glutamate 1, succinate 5 (substrates where indicated), 0.5 mg/ml bovine serum albumin (fatty acid-free), pH 7.25, 50 μM A_p5A, and 2 μM Magnesium Green $5K^+$ salt. Magnesium Green (MgG) fluorescence was recorded in a F-4500 spectrofluorimeter (“Hitachi”, Japan) at 5 Hz acquisition rate, using 506 and 531 nm excitation and emission wavelengths, respectively. Experiments were performed at 37 °C. At the end of each experiment, minimum fluorescence (F_{min}) was measured after addition of 4 mM EDTA, followed by the recording of maximum fluorescence (F_{max}) elicited by addition of 20 mM $MgCl_2$. Free Mg^{2+} concentration (Mg^{2+}_f) was calculated from the equation: $Mg^{2+}_f = (K_d(F-F_{min})/(F_{max}-F))-0.055$ mM, assuming a K_d of 0.9 mM for the MgG-Mg^{2+} complex [76]. The correction term -0.055 mM is empirical, and possibly reflects chelation of other ions by EDTA that have an affinity for MgG, and alter its fluorescence. ADP-ATP exchange rate was estimated using the recently described method by Chinopoulos et al [20], exploiting the differential affinity of ADP and ATP to Mg^{2+}. The rate of ATP appearing in the medium following addition of ADP to energized mitochondria (or *vice versa* in case of deenergized mitochondria), is calculated from the measured rate of change in free extramitochondrial $[Mg^{2+}]$ using the following equation:

$$[\mathrm{ATP}]_t = \left(\frac{\left[\mathrm{Mg}^{2+}\right]_t}{\left[\mathrm{Mg}^{2+}\right]_f} - 1 - \frac{[\mathrm{ADP}]_t\,(t=0) + [\mathrm{ATP}]_t\,(t=0)}{K_{\mathrm{ADP}} + \left[\mathrm{Mg}^{2+}\right]_f} \right) \Big/ \left(\frac{1}{K_{\mathrm{ATP}} + \left[\mathrm{Mg}^{2+}\right]_f} - \frac{1}{K_{\mathrm{ADP}} + \left[\mathrm{Mg}^{2+}\right]_f} \right) \quad \text{(Eq. 3)}$$

Here, $[ADP]_t$ and $[ATP]_t$ are the total concentrations of ADP and ATP, respectively, in the medium, and $[ADP]_t(t=0)$ and $[ATP]_t(t=0)$ are $[ADP]_t$ and $[ATP]_t$ in the medium at time zero. The assay is designed such that the ANT is the sole mediator of changes in $[Mg^{2+}]$ in the extramitochondrial volume, as a result of ADP-ATP exchange [20]. For the calculation of [ATP] or [ADP] from free $[Mg^{2+}]$, the apparent K_d values are identical to those in [20] due to identical experimental conditions (K_{ADP}=0.906 ± 0.023 mM, and K_{ATP}=0.114 ± 0.005 mM). $[Mg^{2+}]_t$ is the total amount of Mg^2 present in the media, i.e. 0.5 mM. Equation 3 (termed ANT calculator) is available for download as an executable file at: http://www.tinyurl.com/ANT-calculator. In case of permeabilized mitochondria by alamethicin, the ATP hydrolysis rate by the F_0F_1-ATP synthase was estimated by the same principle, since one molecule of ATP hydrolyzed yields one molecule of ADP (plus P_i). The rates of ATP efflux, influx and hydrolysis have been estimated sequentially from the same mitochondria, i.e. first mitochondria were energized, a small amount of uncoupler was added, then ADP was added, and ATP efflux was recorded; 150 sec later, 1 μM of SF 6847 was added, and ATP influx was recorded; after 150 sec, alamethicin was added, and ATP hydrolysis by the F_0F_1-ATP synthase was recorded. F_{min} and F_{max} were subsequently recorded as detailed above. For conversion of calibrated free $[Mg^{2+}]$ to free ADP and ATP appearing in the medium, the initial values of total ADP and Mg^{2+} was considered, since free [ADP] and free [ATP] are added parameters in the numerator of Eq. 3.

Mitochondrial membrane potential (ΔΨm) determination in isolated mitochondria

ΔΨm was estimated fluorimetrically with safranine O [77]. Mitochondria (1 mg) were added to 2 ml of incubation medium containing (in mM): KCl 8, K-gluconate 110, NaCl 10, Hepes 10, KH_2PO_4 10 (where indicated), EGTA 0.005, mannitol 10, $MgCl_2$ 0.5 (or 1 where indicated), glutamate 1, succinate 5 (substrates where indicated), 0.5 mg/ml bovine serum albumin (fatty acid-free), pH 7.25, 50 μM A_p5A, and 10 μM safranine O. Fluorescence was recorded in a Hitachi F-4500 spectrofluorimeter at a 5 Hz acquisition rate, using 495 and 585 nm excitation and emission wavelengths, respectively. Experiments were performed at 37 °C. In order to convert safranine O fluorescence into millivolts, a voltage-fluorescence calibration curve was constructed. To this end, safranine O fluorescence was recorded in the presence of 2 nM valinomycin and stepwise increasing K^+ (in the 0.2-120 mM range) which allowed calculation of ΔΨm by the Nernst equation assuming a matrix K^+=120 mM [77].

Mitochondrial matrix pH (pH_i) determination

pH_i of liver mitochondria from WT and CYPD KO mice was estimated as described previously [78], with minor modifications. Briefly, mitochondria (20 mg) were suspended in a 2 ml medium containing (in mM): 225 mannitol, 75 sucrose, 5 Hepes, and 0.1 EGTA (pH=7.4 using Trizma) and incubated with 50 μM BCECF-AM at 30 °C. After 20 min, mitochondria were centrifuged at 10,600 g for 3 min (at 4 °C), washed once and re-centrifuged. The final pellet was suspended in 0.2 ml of the same medium and kept on ice until further manipulation. Fluorescence of hydrolyzed BCECF trapped in the matrix was measured in a Hitachi F-4500 spectrofluorimeter in a ratiometric mode at a 2 Hz acquisition rate, using 450/490 nm excitation and 531 nm emission wavelengths, respectively. Buffer composition and temperature were identical to that used for both $\Delta\Psi_m$ and Mg^{2+} fluorescence determinations (see above). BCECF signal was calibrated using a range of buffers of known pH in the 6.8-7.8 range, and by equilibrating matrix pH to that of the experimental volume by 250 nM SF 6847 plus 1 μM nigericin. For converting BCECF fluorescence ratio to pH we fitted the function: f=a*exp(b/(x+c)) to BCECF fluorescence ratio values. ‘x’ is for BCECF fluorescence ratio, ‘a’, ‘b’ and ‘c’ are constants and ‘f’ represents calculated pH. The fitting of the above function to BCECF fluorescence ratio values obtained by subjecting mitochondria to buffers of known pH returned r^2 >0.99 and

the standard error of the estimates of 'a' and 'c' constants were in the 0.07-0.01 range, and for 'b' < 0.1.

Mitochondrial oxygen consumption

Mitochondrial respiration was recorded at 37 °C with a Clark-type oxygen electrode (Hansatech, UK). Mitochondria (1 mg) were added to 2 ml of an incubation medium containing (in mM): KCl 8, K-gluconate 110, NaCl 10, Hepes 10, KH_2PO_4 10 (where indicated), EGTA 0.005, mannitol 10, $MgCl_2$ 0.5, glutamate 1, succinate 5 (substrates where indicated), 0.5 mg/ml bovine serum albumin (fatty acid-free), pH 7.25, and 50 μM A_p5A. State 3 respiration was initiated by the addition of 0.1-2 mM K^+-ADP (as indicated) to the incubation medium.

Cross-linking, co-precipitation and western blotting

Mitochondria (5 mg/ml) were suspended in the same buffer as for ADP-ATP exchange rates determination and supplemented with succinate (5 mM) and glutamate (1 mM). Cyclosporin A (1 μM) were added where indicated. After 3 min of incubation at 37 °C, 2.5 mM DSP was added, and mitochondria were incubated further for 15 min. Subsequently, mitochondria were sedimented at 10,000 × g for 10 min, and resuspended in 1% digitonin, in a buffer containing 50 mM Trizma, 50 mM KCl, pH 7.6. Samples were then incubated overnight under wheel rotation at 4 °C in the presence of anti-complex V monoclonal antibody covalently linked to protein G-agarose beads (MS501 immunocapture kit, Mitosciences, Eugene, Oregon 97403, USA). After centrifugation at 2,000 × g for 5 min, the beads were washed twice for 5 min in a solution containing 0.05% (w/v) DDM in phosphate-buffered saline. The elution was performed in 1% (w/v) sodium dodecyl sulfate (SDS) for 15 min. To reduce the DSP disulfide bond, the cross-linked immunoprecipitates were treated with 150 mM dithiothreitol (DTT) for 30 min at 37 °C and separated by sodium dodecyl sulfate – polyacrylamide gel electrophoresis (SDS-PAGE). Separated proteins were transferred to a methanol-activated polyvinylidene difluoride membrane. Immunoblotting was performed as recommended by the manufacturers of the antibodies. Mouse monoclonal anti-CYPD (MSA04, Mitosciences) and anti-β subunit of the F_0F_1-ATP synthase (MS503, Mitosciences) primary antibodies were used at concentrations of 2 μg/ml. Immunoreactivity was detected using the appropriate peroxidase-linked secondary antibody (1:4,000, donkey anti-mouse, Jackson Immunochemicals Europe Ltd, Cambridgeshire, UK) and enhanced chemiluminescence detection reagent (RapidStep ECL reagent, Calbiochem, Merck Chemicals, Darmstadt, Germany).

Reagents

Standard laboratory chemicals, P1,P5-Di(adenosine-5′) pentaphosphate (A_p5A), safranine O, nigericin and valinomycin were from Sigma. SF 6847 was from Biomol (BIOMOL GmbH, Hamburg, Germany). DSP was from Piercenet (Thermo Fisher Scientific, Rockford, IL, USA). Magnesium Green $5K^+$ salt and BCECF-AM were from Invitrogen. All mitochondrial substrate stock solutions were dissolved in bi-distilled water and titrated to pH=7.0 with KOH. ATP and ADP were purchased as K^+ salts of the highest purity available and titrated to pH=6.9 with KOH.

Statistics

Data are presented as mean ± SEM; significant differences between groups of data were evaluated by one way ANOVA followed by Tukey's *posthoc* analysis, with $p < 0.05$ considered significant.

Acknowledgments

We are grateful to Dr. Oleg Demin for valuable theoretical advice. This work was supported by the Országos Tudományos Kutatási Alapprogram-Nemzeti Kutatási és Technológiai Hivatal (OTKA-NKTH) grant NF68294 and OTKA NNF78905 grant and Egeszsegügyi Tudományos Tanács (ETT) grant 55160 to C.C. and the NIH grant 1R21NS065396-01 to A.A.S.

References

1. Haworth RA, Hunter DR. The Ca2+-induced membrane transition in mitochondria. II. Nature of the Ca2+ trigger site. Arch Biochem Biophys. 1979; 195:460–467. [PubMed: 38751]
2. Hunter DR, Haworth RA. The Ca2+-induced membrane transition in mitochondria. III. Transitional Ca2+ release. Arch Biochem Biophys. 1979; 195:468–477. [PubMed: 112926]
3. Wang P, Heitman J. The cyclophilins. Genome Biol. 2005; 6:226. [PubMed: 15998457]
4. Baines CP, Kaiser RA, Purcell NH, Blair NS, Osinska H, Hambleton MA, Brunskill EW, Sayen MR, Gottlieb RA, Dorn GW, Robbins J, Molkentin JD. Loss of cyclophilin D reveals a critical role for mitochondrial permeability transition in cell death. Nature. 2005; 434:658–662. [PubMed: 15800627]
5. Nakagawa T, Shimizu S, Watanabe T, Yamaguchi O, Otsu K, Yamagata H, Inohara H, Kubo T, Tsujimoto Y. Cyclophilin D-dependent mitochondrial permeability transition regulates some necrotic but not apoptotic cell death. Nature. 2005; 434:652–658. [PubMed: 15800626]
6. Schinzel AC, Takeuchi O, Huang Z, Fisher JK, Zhou Z, Rubens J, Hetz C, Danial NN, Moskowitz MA, Korsmeyer SJ. Cyclophilin D is a component of mitochondrial permeability transition and mediates neuronal cell death after focal cerebral ischemia. Proc Natl Acad Sci U S A. 2005; 102:12005–12010. [PubMed: 16103352]
7. Basso E, Fante L, Fowlkes J, Petronilli V, Forte MA, Bernardi P. Properties of the permeability transition pore in mitochondria devoid of Cyclophilin D. J Biol Chem. 2005; 280:18558–18561. [PubMed: 15792954]
8. Basso E, Petronilli V, Forte MA, Bernardi P. Phosphate is essential for inhibition of the mitochondrial permeability transition pore by cyclosporin A and by cyclophilin D ablation. J Biol Chem. 2008; 283:26307–26311. [PubMed: 18684715]
9. Lin DT, Lechleiter JD. Mitochondrial targeted cyclophilin D protects cells from cell death by peptidyl prolyl isomerization. J Biol Chem. 2002; 277:31134–31141. [PubMed: 12077116]
10. Scorrano L, Nicolli A, Basso E, Petronilli V, Bernardi P. Two modes of activation of the permeability transition pore: the role of mitochondrial cyclophilin. Mol Cell Biochem. 1997; 174:181–184. [PubMed: 9309684]
11. Luvisetto S, Basso E, Petronilli V, Bernardi P, Forte M. Enhancement of anxiety, facilitation of avoidance behavior, and occurrence of adult-onset obesity in mice lacking mitochondrial cyclophilin D. Neuroscience. 2008; 155:585–596. [PubMed: 18621101]
12. Jobe SM, Wilson KM, Leo L, Raimondi A, Molkentin JD, Lentz SR, Di PJ. Critical role for the mitochondrial permeability transition pore and cyclophilin D in platelet activation and thrombosis. Blood. 2008; 111:1257–1265. [PubMed: 17989312]
13. Du H, Guo L, Fang F, Chen D, Sosunov AA, McKhann GM, Yan Y, Wang C, Zhang H, Molkentin JD, Gunn-Moore FJ, Vonsattel JP, Arancio O, Chen JX, Yan SD. Cyclophilin D deficiency attenuates mitochondrial and neuronal perturbation and ameliorates learning and memory in Alzheimer's disease. Nat Med. 2008; 14:1097–1105. [PubMed: 18806802]
14. Millay DP, Sargent MA, Osinska H, Baines CP, Barton ER, Vuagniaux G, Sweeney HL, Robbins J, Molkentin JD. Genetic and pharmacologic inhibition of mitochondrial-dependent necrosis attenuates muscular dystrophy. Nat Med. 2008; 14:442–447. [PubMed: 18345011]
15. Palma E, Tiepolo T, Angelin A, Sabatelli P, Maraldi NM, Basso E, Forte MA, Bernardi P, Bonaldo P. Genetic ablation of cyclophilin D rescues mitochondrial defects and prevents muscle apoptosis in collagen VI myopathic mice. Hum Mol Genet. 2009; 18:2024–2031. [PubMed: 19293339]
16. Irwin WA, Bergamin N, Sabatelli P, Reggiani C, Megighian A, Merlini L, Braghetta P, Columbaro M, Volpin D, Bressan GM, Bernardi P, Bonaldo P. Mitochondrial dysfunction and apoptosis in myopathic mice with collagen VI deficiency. Nat Genet. 2003; 35:367–371. [PubMed: 14625552]

17. Tiepolo T, Angelin A, Palma E, Sabatelli P, Merlini L, Nicolosi L, Finetti F, Braghetta P, Vuagniaux G, Dumont JM, Baldari CT, Bonaldo P, Bernardi P. The cyclophilin inhibitor Debio 025 normalizes mitochondrial function, muscle apoptosis and ultrastructural defects in Col6a1-/- myopathic mice. Br J Pharmacol. 2009; 157:1045–1052. [PubMed: 19519726]
18. Merlini L, Angelin A, Tiepolo T, Braghetta P, Sabatelli P, Zamparelli A, Ferlini A, Maraldi NM, Bonaldo P, Bernardi P. Cyclosporin A corrects mitochondrial dysfunction and muscle apoptosis in patients with collagen VI myopathies. Proc Natl Acad Sci U S A. 2008; 105:5225–5229. [PubMed: 18362356]
19. Giorgio V, Bisetto E, Soriano ME, Dabbeni-Sala F, Basso E, Petronilli V, Forte MA, Bernardi P, Lippe G. Cyclophilin D Modulates Mitochondrial F0F1-ATP Synthase by Interacting with the Lateral Stalk of the Complex. J Biol Chem. 2009; 284:33982–33988. [PubMed: 19801635]
20. Chinopoulos C, Vajda S, Csanady L, Mandi M, Mathe K, Adam-Vizi V. A novel kinetic assay of mitochondrial ATP-ADP exchange rate mediated by the ANT. Biophys J. 2009; 96:2490–2504. [PubMed: 19289073]
21. Chinopoulos C, Adam-Vizi V. Mitochondria as ATP consumers in cellular pathology. Biochim Biophys Acta. 2010; 1802:221–227. [PubMed: 19715757]
22. Metelkin E, Demin O, Kovacs Z, Chinopoulos C. Modeling of ATP-ADP steady-state exchange rate mediated by the adenine nucleotide translocase in isolated mitochondria. FEBS J. 2009; 276:6942–6955. [PubMed: 19860824]
23. Chinopoulos C, Gerencser AA, Mandi M, Mathe K, Torocsik B, Doczi J, Turiak L, Kiss G, Konrad C, Vajda S, Vereczki V, Oh RJ, Adam-Vizi V. Forward operation of adenine nucleotide translocase during F0F1-ATPase reversal: critical role of matrix substrate-level phosphorylation. FASEB J. 2010; 24:2405–2416. [PubMed: 20207940]
24. Klingenberg M. The ADP and ATP transport in mitochondria and its carrier. Biochim Biophys Acta. 2008; 1778:1978–2021. [PubMed: 18510943]
25. Klingenberg M. The ADP-ATP translocation in mitochondria, a membrane potential controlled transport. J Membr Biol. 1980; 56:97–105. [PubMed: 7003152]
26. Kramer R, Klingenberg M. Modulation of the reconstituted adenine nucleotide exchange by membrane potential. Biochemistry. 1980; 19:556–560. [PubMed: 6243950]
27. Metelkin E, Goryanin I, Demin O. Mathematical modeling of mitochondrial adenine nucleotide translocase. Biophys J. 2006; 90:423–432. [PubMed: 16239329]
28. Dennis SC, Lai JC, Clark JB. Comparative studies on glutamate metabolism in synpatic and non-synaptic rat brain mitochondria. Biochem J. 1977; 164:727–736. [PubMed: 883964]
29. Konig T, Nicholls DG, Garland PB. The inhibition of pyruvate and Ls(+)-isocitrate oxidation by succinate oxidation in rat liver mitochondria. Biochem J. 1969; 114:589–596. [PubMed: 4309530]
30. Quagliariello E, PAPA S, SACCONE C, Palmieri F, FRANCAVILLA A. THE OXIDATION OF GLUTAMATE BY RAT-LIVER MITOCHONDRIA. Biochem J. 1965; 95:742–748. [PubMed: 14342510]
31. Demin OV, Westerhoff HV, Kholodenko BN. Mathematical modelling of superoxide generation with the bc1 complex of mitochondria. Biochemistry (Mosc). 1998; 63:634–649. [PubMed: 9668203]
32. Demin OV, Gorianin II, Kholodenko BN, Westerhoff HV. Kinetic modeling of energy metabolism and generation of active forms of oxygen in hepatocyte mitochondria. Mol Biol (Mosk). 2001; 35:1095–1104. [PubMed: 11771135]
33. Nicholls, DG.; Ferguson, SJ. Bioenergetics. 3. Academic Press; 2002.
34. Wilson DF, Owen CS, Erecinska M. Quantitative dependence of mitochondrial oxidative phosphorylation on oxygen concentration: a mathematical model. Arch Biochem Biophys. 1979; 195:494–504. [PubMed: 224820]
35. Arnold S, Kadenbach B. Cell respiration is controlled by ATP, an allosteric inhibitor of cytochrome-c oxidase. Eur J Biochem. 1997; 249:350–354. [PubMed: 9363790]
36. Moreno-Sanchez R, Devars S, Lopez-Gomez F, Uribe A, Corona N. Distribution of control of oxidative phosphorylation in mitochondria oxidizing NAD-linked substrates. Biochim Biophys Acta. 1991; 1060:284–292. [PubMed: 1751513]

37. Lopez-Gomez FJ, Torres-Marquez ME, Moreno-Sanchez R. Control of oxidative phosphorylation in AS-30D hepatoma mitochondria. Int J Biochem. 1993; 25:373–377. [PubMed: 8096469]
38. Wisniewski E, Kunz WS, Gellerich FN. Phosphate affects the distribution of flux control among the enzymes of oxidative phosphorylation in rat skeletal muscle mitochondria. J Biol Chem. 1993; 268:9343–9346. [PubMed: 8486629]
39. Tager JM, Wanders RJ, Groen AK, Kunz W, Bohnensack R, Kuster U, Letko G, Bohme G, Duszynski J, Wojtczak L. Control of mitochondrial respiration. FEBS Lett. 1983; 151:1–9. [PubMed: 6337871]
40. Kunz W, Gellerich FN, Schild L, Schonfeld P. Kinetic limitations in the overall reaction of mitochondrial oxidative phosphorylation accounting for flux-dependent changes in the apparent delta GexP/delta mu H+ ratio. FEBS Lett. 1988; 233:17–21. [PubMed: 2898384]
41. Hale DE, Williamson JR. Developmental changes in the adenine nucleotide translocase in the guinea pig. J Biol Chem. 1984; 259:8737–8742. [PubMed: 6086610]
42. Tiivel T, Kadaya L, Kuznetsov A, Kaambre T, Peet N, Sikk P, Braun U, Ventura-Clapier R, Saks V, Seppet EK. Developmental changes in regulation of mitochondrial respiration by ADP and creatine in rat heart in vivo. Mol Cell Biochem. 2000; 208:119–128. [PubMed: 10939635]
43. Brand MD, Hafner RP, Brown GC. Control of respiration in non-phosphorylating mitochondria is shared between the proton leak and the respiratory chain. Biochem J. 1988; 255:535–539. [PubMed: 2849419]
44. Kay L, Nicolay K, Wieringa B, Saks V, Wallimann T. Direct evidence for the control of mitochondrial respiration by mitochondrial creatine kinase in oxidative muscle cells in situ. J Biol Chem. 2000; 275:6937–6944. [PubMed: 10702255]
45. Groen AK, Wanders RJ, Westerhoff HV, van der MR, Tager JM. Quantification of the contribution of various steps to the control of mitochondrial respiration. J Biol Chem. 1982; 257:2754–2757. [PubMed: 7061448]
46. Kholodenko BN. Control of mitochondrial oxidative phosphorylation. J Theor Biol. 1984; 107:179–188. [PubMed: 6717037]
47. Schonfeld P, Bohnensack R. Developmental changes of the adenine nucleotide translocation in rat brain. Biochim Biophys Acta. 1995; 1232:75–80. [PubMed: 7495839]
48. Wisniewski E, Gellerich FN, Kunz WS. Distribution of flux control among the enzymes of mitochondrial oxidative phosphorylation in calcium-activated saponin-skinned rat musculus soleus fibers. Eur J Biochem. 1995; 230:549–554. [PubMed: 7607228]
49. Hafner RP, Brown GC, Brand MD. Analysis of the control of respiration rate, phosphorylation rate, proton leak rate and protonmotive force in isolated mitochondria using the ‘top-down’ approach of metabolic control theory. Eur J Biochem. 1990; 188:313–319. [PubMed: 2156698]
50. Chance, B.; Estabrook, RW.; Williamson, JR. Control of energy metabolism. Academic Press; New York: 1965.
51. Kacser, H.; Burns, JA. Rate control of biological processes. Cambridge University Press; London: 1973.
52. Kacser H, Burns JA. MOlecular democracy: who shares the controls? Biochem Soc Trans. 1979; 7:1149–1160. [PubMed: 389705]
53. Heinrich R, Rapoport TA. A linear steady-state treatment of enzymatic chains. General properties, control and effector strength. Eur J Biochem. 1974; 42:89–95. [PubMed: 4830198]
54. PULLMAN ME, MONROY GC. A NATURALLY OCCURRING INHIBITOR OF MITOCHONDRIAL ADENOSINE TRIPHOSPHATASE. J Biol Chem. 1963; 238:3762–3769. [PubMed: 14109217]
55. Campanella M, Casswell E, Chong S, Farah Z, Wieckowski MR, Abramov AY, Tinker A, Duchen MR. Regulation of mitochondrial structure and function by the F1Fo-ATPase inhibitor protein, IF1. Cell Metab. 2008; 8:13–25. [PubMed: 18590689]
56. Rouslin W, Broge CW. IF1 function in situ in uncoupler-challenged ischemic rabbit, rat, and pigeon hearts. J Biol Chem. 1996; 271:23638–23641. [PubMed: 8798581]
57. Rouslin W, Broge CW. Factors affecting the species-homologous and species-heterologous binding of mitochondrial ATPase inhibitor, IF1, to the mitochondrial ATPase of slow and fast heart-rate hearts. Arch Biochem Biophys. 1993; 303:443–450. [PubMed: 8512326]

58. Klingenberg M, Rottenberg H. Relation between the gradient of the ATP/ADP ratio and the membrane potential across the mitochondrial membrane. Eur J Biochem. 1977; 73:125–130. [PubMed: 14003]
59. Chance B, Mela L. Hydrogen ion concentration changes in mitochondrial membranes. J Biol Chem. 1966; 241:4588–4599. [PubMed: 5926170]
60. Petronilli V, Cola C, Bernardi P. Modulation of the mitochondrial cyclosporin A-sensitive permeability transition pore. II. The minimal requirements for pore induction underscore a key role for transmembrane electrical potential, matrix pH, and matrix Ca2+ J Biol Chem. 1993; 268:1011–1016. [PubMed: 7678245]
61. Vajda S, Mandi M, Konrad C, Kiss G, Ambrus A, Adam-Vizi V, Chinopoulos C. A re-evaluation of the role of matrix acidification in uncoupler-induced Ca2+ release from mitochondria. FEBS J. 2009; 276:2713–2724. [PubMed: 19459934]
62. Chinopoulos C, Adam-Vizi V. Mitochondrial Ca(2+)sequestration and precipitation revisited. FEBS J. 2010; 277:3637–3651. [PubMed: 20659160]
63. Dominguez-Ramirez L, Gomez-Puyou A, De Gomez-Puyou MT. A hinge of the endogeneous ATP synthase inhibitor protein: the link between inhibitory and anchoring domains. Proteins. 2006; 65:999–1007. [PubMed: 17019684]
64. Bisetto E, Di PF, Simula MP, Mavelli I, Lippe G. Mammalian ATPsynthase monomer versus dimer profiled by blue native PAGE and activity stain. Electrophoresis. 2007; 28:3178–3185. [PubMed: 17703470]
65. ter Welle HF, Slater EC. Uncoupling of respiratory-chain phosphorylation by arsenate. Biochim Biophys Acta. 1967; 143:1–17. [PubMed: 4227788]
66. CRANE RK, LIPMANN F. The effect of arsenate on aerobic phosphorylation. J Biol Chem. 1953; 201:235–243. [PubMed: 13044791]
67. WADKINS CL. Stimulation of adenosine triphosphatase activity of mitochondria and submitochondrial particles by arsenate. J Biol Chem. 1960; 235:3300–3303. [PubMed: 13782426]
68. Duee ED, Vignais PV. Kinetics of phosphorylation of intramitochondrial and extramitochondrial adenine nucleotides as related to nucleotide translocation. J Biol Chem. 1969; 244:3932–3940. [PubMed: 4979772]
69. Brand MD, Harper ME, Taylor HC. Control of the effective P/O ratio of oxidative phosphorylation in liver mitochondria and hepatocytes. Biochem J. 1993; 291(Pt 3):739–748. [PubMed: 8489502]
70. Woodfield K, Ruck A, Brdiczka D, Halestrap AP. Direct demonstration of a specific interaction between cyclophilin-D and the adenine nucleotide translocase confirms their role in the mitochondrial permeability transition. Biochem J. 1998; 336(Pt 2):287–290. [PubMed: 9820802]
71. Bernardi P. Modulation of the mitochondrial cyclosporin A-sensitive permeability transition pore by the proton electrochemical gradient. Evidence that the pore can be opened by membrane depolarization. J Biol Chem. 1992; 267:8834–8839. [PubMed: 1374381]
72. Petronilli V, Cola C, Massari S, Colonna R, Bernardi P. Physiological effectors modify voltage sensing by the cyclosporin A-sensitive permeability transition pore of mitochondria. J Biol Chem. 1993; 268:21939–21945. [PubMed: 8408050]
73. Scorrano L, Petronilli V, Bernardi P. On the voltage dependence of the mitochondrial permeability transition pore. A critical appraisal. J Biol Chem. 1997; 272:12295–12299. [PubMed: 9139672]
74. Tyler DD, Gonze J. Methods Enzymol. 1967; 10:75–77.
75. Smith PK, Krohn RI, Hermanson GT, Mallia AK, Gartner FH, Provenzano MD, Fujimoto EK, Goeke NM, Olson BJ, Klenk DC. Measurement of protein using bicinchoninic acid. Anal Biochem. 1985; 150:76–85. [PubMed: 3843705]
76. Leyssens A, Nowicky AV, Patterson L, Crompton M, Duchen MR. The relationship between mitochondrial state, ATP hydrolysis, [Mg2+]i and [Ca2+]i studied in isolated rat cardiomyocytes. J Physiol. 1996; 496(Pt 1):111–128. [PubMed: 8910200]
77. Akerman KE, Wikstrom MK. Safranine as a probe of the mitochondrial membrane potential. FEBS Lett. 1976; 68:191–197. [PubMed: 976474]
78. Zolkiewska A, Czyz A, Duszynski J, Wojtczak L. Continuous recording of intramitochondrial pH with fluorescent pH indicators: novel probes and limitations of the method. Acta Biochim Pol. 1993; 40:241–250. [PubMed: 8212962]

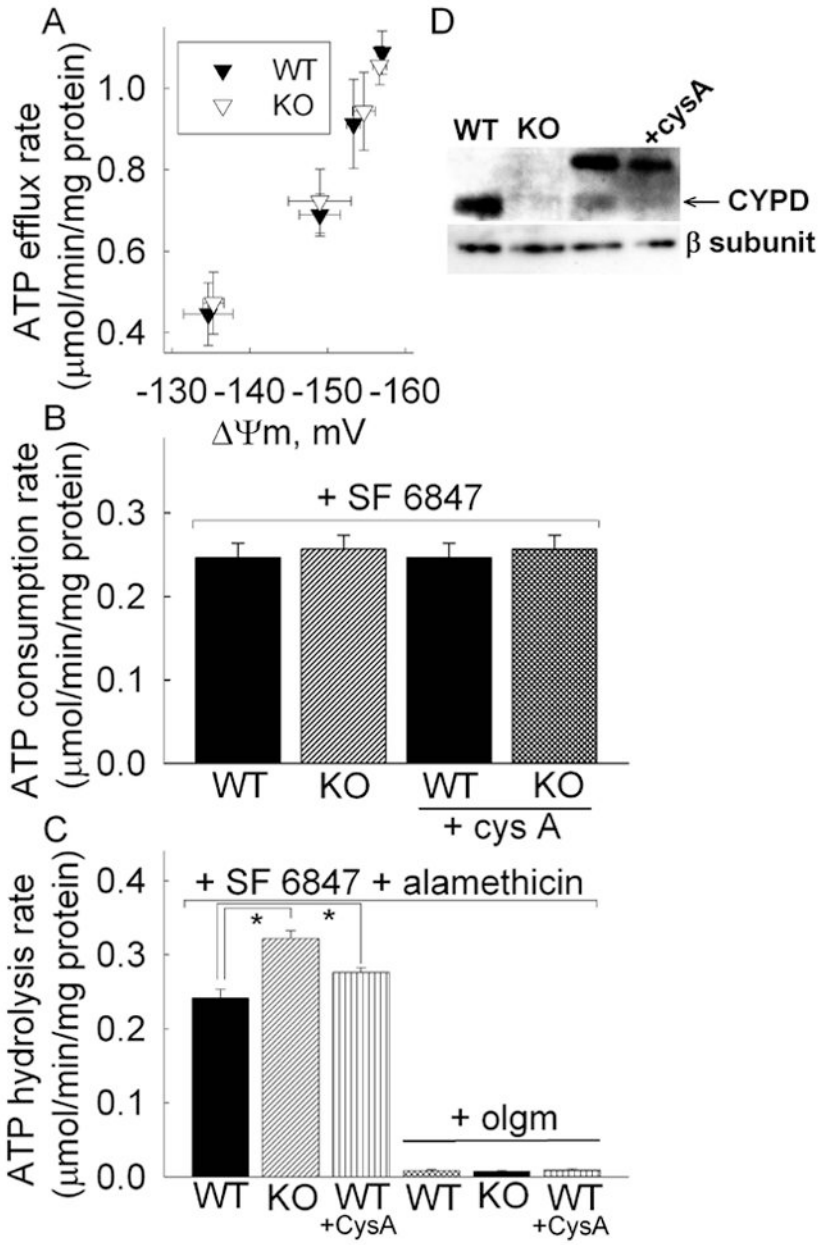

Figure 1. ADP-ATP exchange rates in intact mitochondria and ATP hydrolysis rates in permeabilized mitochondria; CYPD binds on F_0F_1-ATP synthase, in a cys A-inhibitable manner in intact mouse liver mitochondria

A: ATP efflux rates as a function of ΔΨm in intact, energized mouse liver mitochondria isolated from WT and CYPD KO mice. **B**: Bar graphs of ATP consumption rates in intact, completely deenergized WT and CYPD KO mouse liver mitochondria, and effect of cyclosporin A. **C**: Bar graphs of ATP hydrolysis rates in permeabilized WT +/- cys A and CYPD KO mouse liver mitochondria, and effect of oligomycin (olgm). *, significant, (Tukey's test, $p<0.05$). **D**: Lanes 1 and 2 represent CYPD-WT and KO mitochondria respectively (0.85 μgr each). Lanes 3 and 4 represent co-precipitated samples of cross-linked intact mitochondria, treated with 1% digitonin, prior to cross-linking. For lane 4, mitochondria were additionally treated with cys A, prior to cross-linking. Upper panel is a western blot for CYPD, lower panel for the β subunit of F_0F_1-ATP synthase.

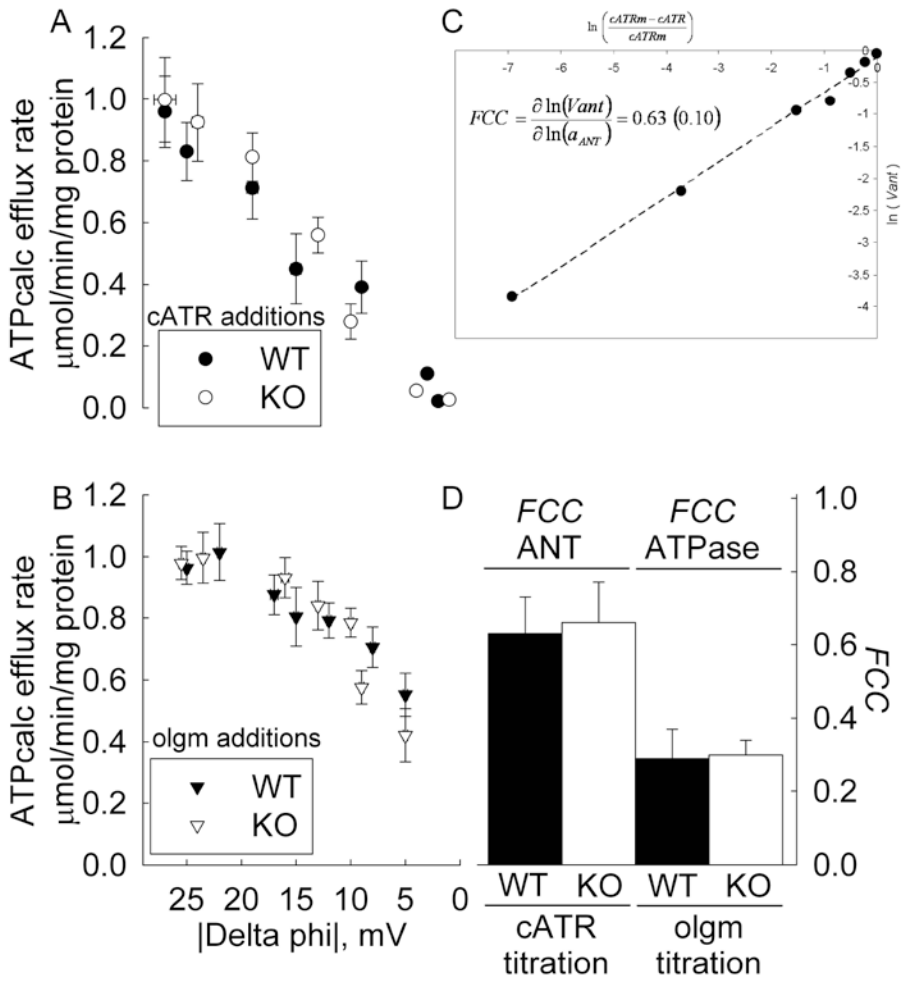

Figure 2. Determination of flux control coefficients of ANT and F_0F_1-ATP synthase for adenine nucleotide flux rates

A: ATP-ADP steady-state exchange rate mediated by ANT as a function of Delta phi, for various carboxyatractyloside (catr) concentrations. The points represent the additions of 0, 40, 80, 120, 160, 200, 240 and 280 nM of catr. Data shown as black circles were obtained from WT liver mitochondria. Data shown as open circles were obtained from CYPD KO liver mitochondria. **B**: ATP-ADP steady-state exchange rate mediated by ANT as a function of Delta phi, for various oligomycin (olgm) concentrations. The points represent the additions of 0, 5, 10, 15, 20, 25, 30 and 35 nM of olgm. Data shown as black triangles were obtained from WT liver mitochondria. Data shown as open triangles were obtained from CYPD KO liver mitochondria. Panels **A** and **B** share the same Delta phi axis. Delta phi represents the difference of ΔΨm before and after addition of 2 mM ADP to liver mitochondria (using 1 mM total $MgCl_2$) pretreated with catr or olgm at the above sub-maximal concentrations. **C**: The dependence of ATP transport flux on ADP-ATP exchange rate mediated by the ANT (log values). The black circles represent the measured values from WT mitochondria, shown in panel **A**. The dashed line represents a linear regression analysis. **D**: Values of flux control coefficients of ANT and F_0F_1-ATP synthase for ADP-ATP exchange rates, for WT and CYPD KO mice mitochondria, calculated by linear regression analysis as depicted in panel **C**, from the data shown in panels **A** and **B**.

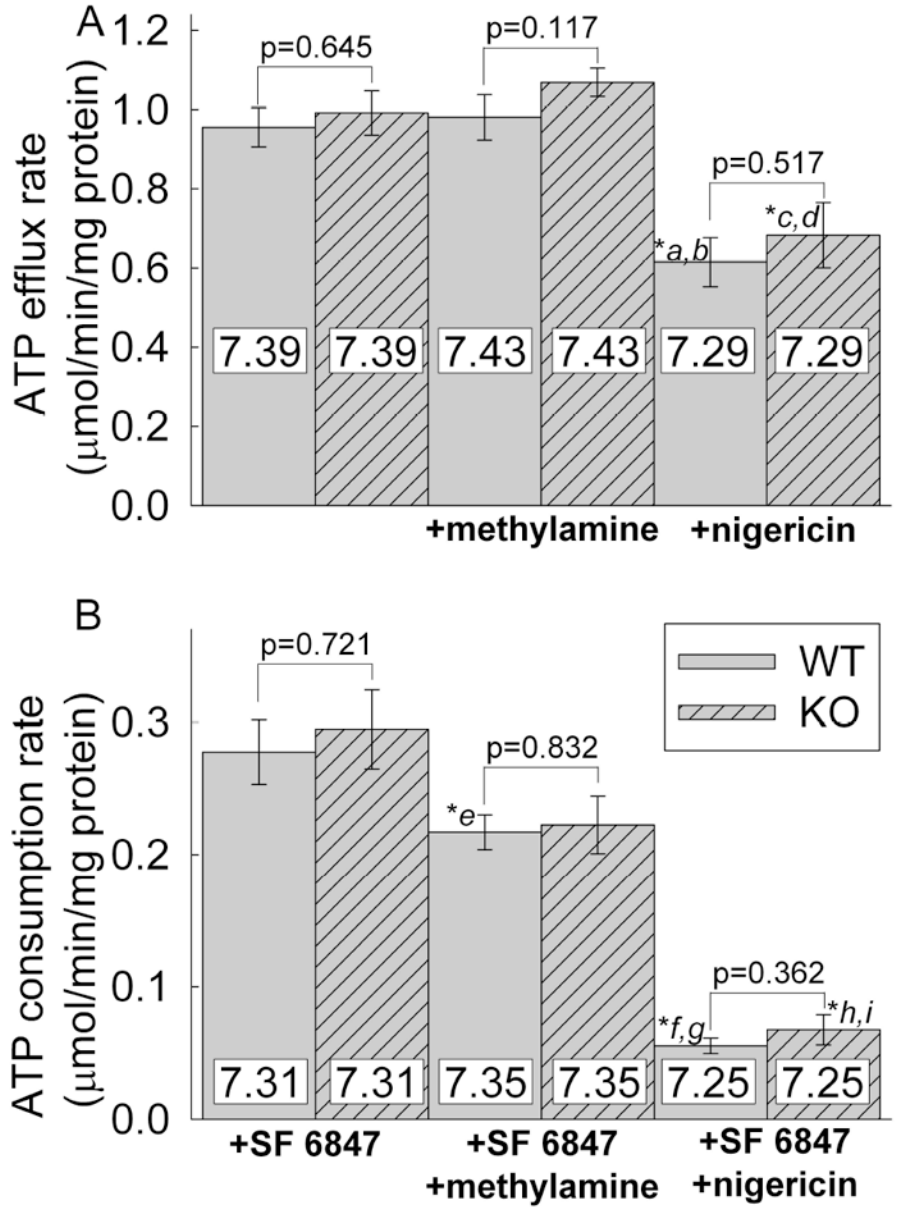

Figure 3. ATP efflux (A) and consumption (B) rates in WT and CYPD KO (striped bars) mitochondria as a function of matrix pH

Matrix pH is shown in the white box within each bar for the respective condition indicated in the x-axis. a*, significant from WT control. b* significant from WT + methylamine. c*, significant from KO control. d* significant from KO + methylamine. e*, significant from WT +SF 6847. f*, significant from WT +SF 6847. g*, significant from WT +SF 6847 + methylamine. h*, significant from KO +SF 6847. i*, significant from KO +SF 6847 + methylamine.

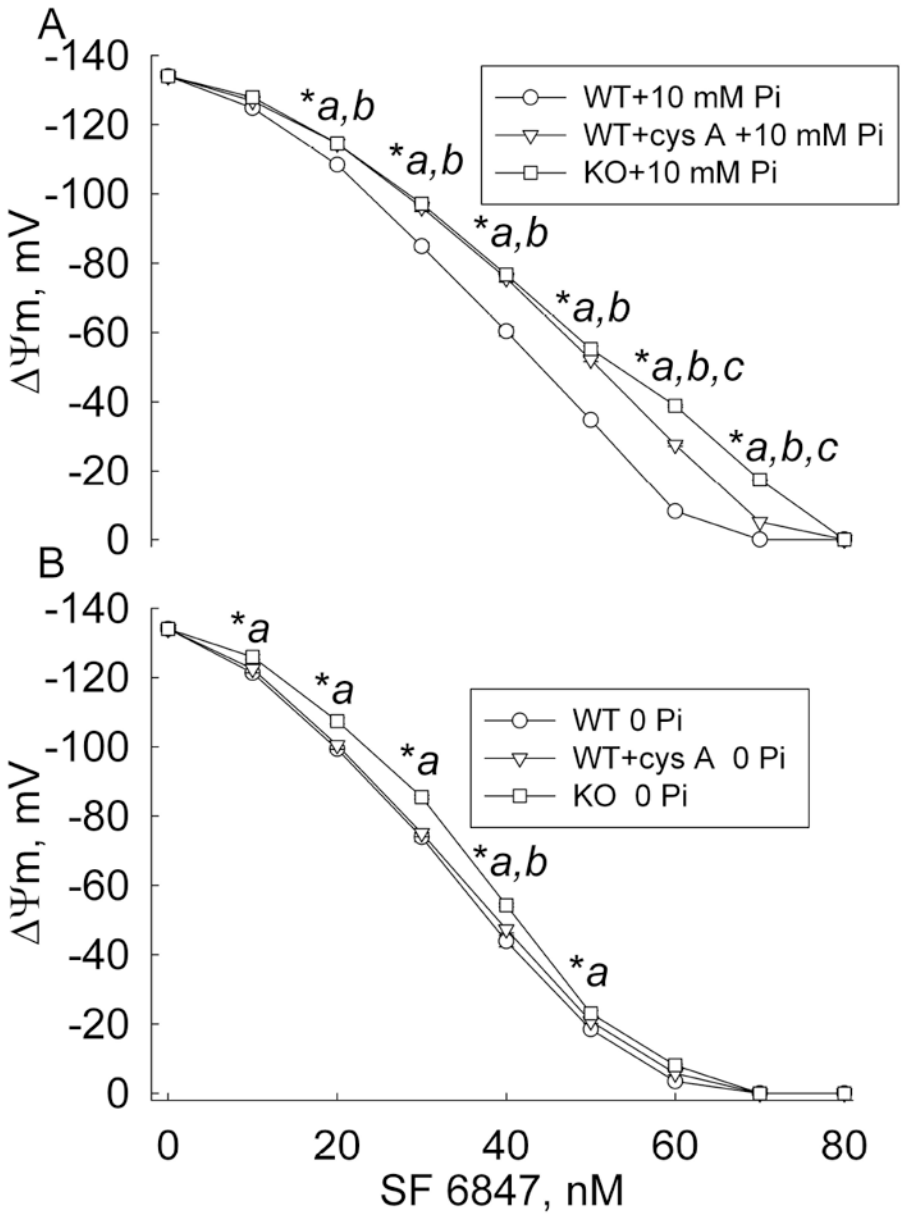

Figure 4. Effect of CYPD on F_0F_1-ATPase-mediated H^+ pumping due to ATP hydrolysis in intact mitochondria

A: Safranine O fluorescence values converted to mV in intact, deenergized WT and CYPD KO mitochondria by substrate deprivation and rotenone, subsequently energized by exogenous addition of 2 mM ATP (with 1 mM total $MgCl_2$ in the buffer), as a function of uncoupler dose (0-80 nM), in the presence of 10 mM P_i in the medium. **B**: same as in **A**, but in the absence of P_i from the medium. *a, statistically significant, KO significantly different from WT; *b, statistically significant, WT +cys A significantly different from WT; *c, statistically significant, KO significantly different from WT+cys A (Tukey's test, $p<0.05$).

Table 1

Estimation of the change (in percentage) in ADP-ATP exchange rate mediated by the ANT as a function of an increase in F_0F_1-ATP synthase activity (in percentage), at different $\Delta\Psi m$ values, for T_o= 1 mM and D_o = 1 mM.

Increase in F_0F_1-ATP synthase activity (%)	**Increase in ADP-ATP exchange rate, mediated by the ANT (%)**				
+30	+1.38	+1.94	+3.65	+7.7	+1.70[a]
$\Delta\Psi m$	-157 mV	-154 mV	-147 mV	-134 mV	0 mV

[a] reverse mode of operation of both ANT and F_0F_1-ATP synthase

Table 2

Effect of CYPD ablation or its inhibition by cyclosporin A on the rates of respiration of mouse liver mitochondria

	Wild type	CYPD KO
State 4	32.0 ± 1.2	30.6 ± 1.0
AsO_4	101.4 ± 3.4[a]	113.1 ± 4.9
Vmax	145.0 ± 7.2	146.4 ± 2.9
ACI	3.2 ± 0.1[b]	3.7 ± 0.2
+CsA, State 4	30.2 ± 1.4	32.0 ± 0.7
+CsA, AsO_4	110.4 ± 4.7[c]	111.6 ± 1.5
+CsA, Vmax	139.5 ± 10.8	147.6 ± 2.6
+CsA, ACI	3.7 ± 0.1[d]	3.5 ± 0.1

a,b **significant difference between wild type and CYPD KO mitochondria, p<0.04 (a) and p<0.02 (b)**, n=7;

c,d significant difference between untreated and Cyclosporin A -treated mitochondria, p<0.03 (**c**) and p<0.001 (**d**), n=6.

ACI - acceptor control index, the rate of respiration in the presence of $ASO4$ divided by the rate of respiration before the addition of $ASO4$. Vmax, the maximum rate of respiration obtained after addition of ADP